TOPICAL REVIEW — Fundamental physics research in lithium batteries

Size effects in lithium ion batteries*

Hu-Rong Yao(姚胡蓉)[1,2], Ya-Xia Yin(殷雅侠)[1], and Yu-Guo Guo (郭玉国)[1,2,3,†]

[1] CAS Key Laboratory of Molecular Nanostructure and Nanotechnology, Institute of Chemistry, Chinese Academy of Sciences, Beijing 100190, China

[2] University of Chinese Academy of Sciences, Beijing 100049, China

[3] Shandong Wina Green Power Co. Ltd., Shouguang 262705, China

(Received 11 May 2015; revised manuscript received 7 July 2015; published online 7 December 2015)

Size-related properties of novel lithium battery materials, arising from kinetics, thermodynamics, and newly discovered lithium storage mechanisms, are reviewed. Complementary experimental and computational investigations of the use of the size effects to modify electrodes and electrolytes for lithium ion batteries are enumerated and discussed together. Size differences in the materials in lithium ion batteries lead to a variety of exciting phenomena. Smaller-particle materials with highly connective interfaces and reduced diffusion paths exhibit higher rate performance than the corresponding bulk materials. The thermodynamics is also changed by the higher surface energy of smaller particles, affecting, for example, secondary surface reactions, lattice parameter, voltage, and the phase transformation mechanism. Newly discovered lithium storage mechanisms that result in superior storage capacity are also briefly highlighted.

Keywords: lithium ion batteries, size effects, experiment, calculation

PACS: 82.47.Aa **DOI:** 10.1088/1674-1056/25/1/018203

1. Introduction

Exciting differences appear in reduced-size materials. The observable differences include a significantly great ratio of surface/interface to volume, excellent enhancement of surface energy, variation of lattice constant, greater defect concentration, and so on. The observable changes mentioned above may cause some magical effects such as the quantum size effect, the coulomb blockade, the quantum tunneling effect, and the dielectric confinement effect. Indeed, these unique size efforts have been studied in multiple fields, including chemistry, physics, biology, electronics, and battery material design. The design of Li ion batteries with excellent performance requires orchestrating knowledge from multiple disciplines. The size effects in Li ion battery materials also alter various battery properties such as the power density.

With the ceaseless development of portable electronics and the deployment of electric vehicles, considerable attention is paid to electrochemical energy storage with high power density. Micrometer-sized electrode materials cannot satisfy the requirements to charge/discharge rapidly due to the poor kinetics. It is well known that the size effects in materials can overcome this restriction by shortening the diffusion lengths of both electrons and Li ions, increasing the area of contact between the electrode and electrolyte, enhancing structural stability, and so on.[1] The inactive materials may even turn to active ones by reducing their sizes. But there are accompanying disadvantages such as low thermodynamic stability and intense side reactions. The superior performance of variously sized Li ion battery materials has attracted widespread attention.

The present review highlights the enhanced performance arising from the reduced particle size, the associated mechanisms, and new lithium storage mechanisms. To provide compelling detail, we will discuss a range of experimental and computational evidences.

2. The experimental perspective

Varying materials' size changes the kinetics and thermodynamics of both electrodes and electrolytes.

2.1. Electrodes

2.1.1. Kinetics

2.1.1.1 Diffusion length

In the kinetic process of Li ion batteries, ion diffusion in the electrode, called the rate-determining step, determines the speed of the primary electrochemical reaction. The relation among the mean diffusion time of Li ions (τ), the diffusion coefficient (D), and the diffusion length (L) is given as

$$\tau = L^2/(2D). \tag{1}$$

It is clear here that the kinetic process can be accelerated by increasing D or decreasing L. The diffusion coefficient can be

*Project supported by the National Natural Science Foundation of China (Grant Nos. 51225204 and 21303222), the Shandong Taishan Scholarship, China, the Ministry of Science and Technology, China (Grant No. 2012CB932900), and the Strategic Priority Research Program of the Chinese Academy of Sciences (Grant No. XDA09010000).

†Corresponding author. E-mail: ygguo@iccas.ac.cn

© 2016 Chinese Physical Society and IOP Publishing Ltd

calculated by the following formula from first principles, according to the transition state theory, the hopping mechanism, and the lattice gas model:

$$D = v_0 l^2 \exp\left(\frac{E_a}{K_B T}\right). \quad (2)$$

Here, v_0 is the Li ion vibration frequency, l is the hopping distance, E_a is the Li ion migration energy barrier, and K_B and T are the Boltzmann constant and the absolute temperature, respectively. The diffusion coefficient D can be improved by either reducing E_a via doping or increasing T via warming. But these tactics may destabilize the structure and reduce the battery safety. In contrast, the diffusion length L can be decreased easily by nanocrystallization of materials, dramatically reducing the diffusion time τ, due to the quadratic relationship between τ and L.

Shortening the diffusion length is commonly used to improve the rate performance of the conventional Li ion battery materials.[2–4] For example, the conventional cathode material $LiFePO_4$ has been studied extensively because of its high theoretical energy density of 580 W·h/kg. However, it suffers from low electronic and ionic conductivities. Wu *et al.* reported that a nanocomposite with highly dispersed nanoparticles of $LiFePO_4$ in a nanoporous carbon matrix can be fully charged or discharged within a period of less than 30 s.[2] The extremely high power is enabled by nanometer-sized $LiFePO_4$ particles, which shorten the Li ion diffusion path, and by quick Li^+/e^- diffusion, which arises from the nature of the nanoporous carbon matrix.[2]

Size reduction not only improves the rate performance of some electrode materials, but also endows some inactive materials such as rutile TiO_2 with electroactivity.[5,6] Rutile is the most stable structure of TiO_2 under standard conditions, but Li insertion into rutile is usually reported to be negligible. The capacity can be significantly improved by nanocrystallization.[5,7,8] Hu *et al.* reported observing high capacity, excellent capacity retention during cycling, and high rate performance for rutile TiO_2 needles about 10 nm in diameter and 30 nm in length.[5]

2.1.1.2 Contact area

Besides the reduced diffusion length, another reason for the higher intercalation/deintercalation rates of some nanomaterials is the increased contact area, which promotes Li ion exchange. The excellent performance of nanoscale $Li_4Ti_5O_{12}$ is a suitable example. $Li_4Ti_5O_{12}$ is an attractive anode material due to its low cost, zero strain, and operating voltage plateau which are sufficient to avoid the formation of lithium dendrites and solid electrolyte interface (SEI). However, it suffers from a moderate Li ion diffusion coefficient and poor electronic conductivity, which is also indicated by the band gap of about 2 eV calculated by *ab initio* study.[9] The nanocrystalline $Li_4Ti_5O_{12}$ prepared by combustion synthesis exhibits high rate capability and good capacity retention, both of which can be attributed to the presence of highly porous nanostructures having BET surface areas of about 12 m^2/g.[10]

The electron exchange can also be improved by enhancing the contact area between the active materials and the conductive additives. Zhang *et al.* improved the effective contact area by connecting one-dimensional carbon nanofibers with zero-dimensional carbon black to build a conductive network, which is established within the $Li_4Ti_5O_{12}$ particles by the penetrating multiple carbon nanofibers, and the carbon black particles attached onto the surface of the $Li_4Ti_5O_{12}$ particles fill in the gaps between them.[11]

The materials with one-dimensional Li diffusion channel may exhibit high rate performance if the orientation of matter is controlled to improve the exposed area with high pore density for Li insertion/extraction.[12]

2.1.1.3 Diffusion coefficient

The diffusion coefficient is also affected by nanocrystallization in some cases. Based on their computational results for $LiFePO_4$, Malik *et al.* suggested that the kinetic benefit of small scale materials results from both shortened transport paths and enhanced diffusion constants of one-dimensional channel materials. The phenomenon will be introduced very briefly in the section below on theoretical calculation.[13]

The dynamic performance of any nanoscale electrodes should be dramatically improved in theory, but it is not actually the case for some electrode materials due to the thermodynamic instability that comes with size reduction.

2.1.2. Thermodynamics

2.1.2.1 Secondary surface reactions

Due to an abundance of dangling bonds, a large surface free energy, a high density of defects, and the high surface-to-volume ratio of nanostructured electrode materials, the risk of secondary reactions is dramatically high, leading to a short life cycle and consuming much of the Li supplied by the cathodes.

Nano $LiCoO_2$ exhibits worse cyclability than bulk $LiCoO_2$ due to the presence of SEI film, formed mainly in spontaneous chemical reactions between the solvent molecules and nanoscale $LiCoO_2$.[14,15] Furthermore, it has been found in many nanostructured transition metal oxides that thick SEI films formed during Li uptake may disappear completely upon Li extraction, which leads to capacity fading and safety problems. Therefore, surface modifications must be considered for nanostructured transition metal oxides. For instance, carbon coated Fe_3O_4 nanospindles exhibit very high specific capacity, superior cycling performance, and high rate performance because the carbon coating enhances electronic conductivity and stabilizes the SEI films.[16]

2.1.2.2 Agglomerate

The abundant agglomerates that lead to the irreversible fading of capacity and shortened cycle life will occur, and they occur during the preparation processes or electrochemical cycling.

Surface coating and the formation of nano/micro hierarchical structures are efficient techniques to avoid agglomeration, on account of the formation of highly dispersed nanocrystals in the matrix.[16,17] For example, Guo *et al.* proposed that a conducting 3D network (a sketch is shown in Fig. 1), a synthesis of a mesoporous TiO_2:RuO_2 nanocomposite, would exhibit optimal high power density because of combining the advantages of nanoscale networks (negligible diffusion time, enhanced local conductivity, and possibly faster phase transfer reactions) and microscopic networks (good stability and ease of fabrication).[17]

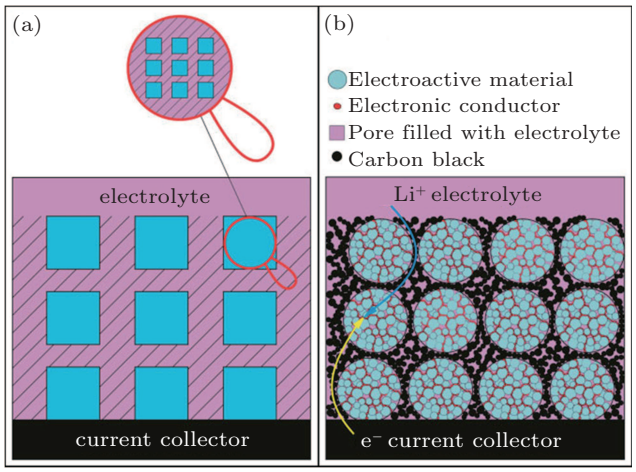


Fig. 1. (a) Schematic of the desired design; the shaded areas represent 3D conductive networks. (b) Sketch of a realistic composite in which Li^+/e^- can transfer to most of the electroactive material particles through the 3D conductive networks.[17]

2.1.2.3 Lattice parameter

Lattice expansion dependent upon particle size is observed in some materials; however, explanations vary, including a change of bond length, a reduction of atomic charge, and so on.[15,18,19] According to magnetic susceptibility measurements, the fact that 20% of the cobalt at the surface layer is Co^{2+} ions can explain the lattice expansion of nanocrystalline $LiCoO_2$, because the Co^{2+}–O distance is longer than the Co^{3+}–O distance.[15] Variation of the lattice parameter also impacts Li ion diffusion kinetics, since it changes the channel size.

2.1.2.4 Voltage

The thermodynamic equilibrium voltage (V) is related to the difference of chemical potential ($\Delta\mu$) between the reactants and products

$$V = -\Delta\mu/F, \tag{3}$$

where F is the Faraday constant. For nano-materials, the defect energy contributed mainly from the surface free energy should be taken into consideration for the chemical potential, as

$$\mu_{\text{nano}} = \mu_{\text{bulk}} + 2V_{\text{m}}(\gamma/r), \tag{4}$$

where V_{m} is the partial molar volume, and γ and r are the effective surface tension and grain radius, respectively. The voltage curve of nanoscale electrodes differs from the voltage curve of the corresponding bulk materials according to the variation of the chemical potential μ. For example, a stable excess electromotive force of about 62 mV was obtained at 621 K for the nanoscale rutile TiO_2 of 25 nm versus 2 μm rutile.[20] Okubo *et al.* explained the difference in discharge curves with reference to the fluctuation of Li ion intercalation site energy originating from the common structure disorder in nanoscale materials.[15] Figure 2 shows the expected discharge curves for bulk and nanocrystalline $LiCoO_2$.[15] Nanoscale materials with two-phase Li insertion/de-insertion processes may exhibit a characteristic voltage behavior.[21,22] Electrodes made of $LiFePO_4$ nanoparticles have sloping voltage charge/discharge curves, a characteristic of single-phase behavior.[21] Zhu *et al.* reported that

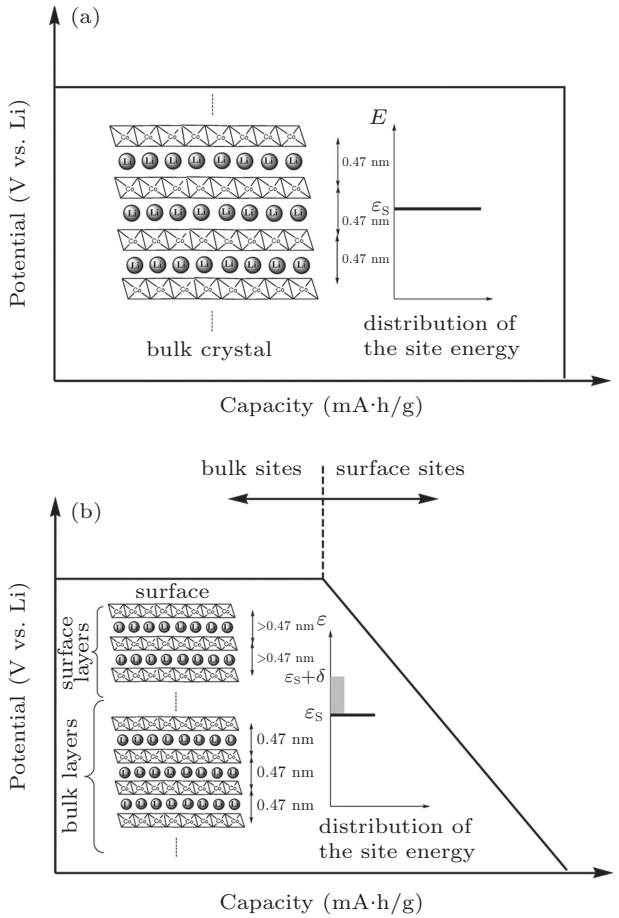


Fig. 2. (a) Structure sketch and expected discharge curve for bulk $LiCoO_2$, in which the site energy is considered to be a constant ε_S. (b) Structure sketch and expected discharge curve for nanoscale $LiCoO_2$. The fluctuation of the site energy is represented by δ.[15]

open circuit voltages decrease with decreasing particle size for nanocrystalline $LiFePO_4$ originating from the variation of lithium potential in this situation, and similar phenomena are observed for amorphous $LiFePO_4$ as well.[22]

2.1.2.5 Morphology

Defect energy not only impacts the thermodynamic equilibrium voltage of a given structure, but also results in the reversal of the stable morphology of a material, like Fe_2O_3. The phase transition from maghemite (γ-Fe_2O_3) to hematite (α-Fe_2O_3) has been observed *in situ* in XRD as the crystal size varies from 9 nm to 16 nm due to the Gibbs-energy change.[23]

2.1.2.6 Phase transition mechanism

Phase transition behavior is also connected with the size of material particles. Varied staging phenomena have been observed in different-sized particles of $LiFePO_4$, which is widely considered to be a typical first-order phase transition material.[24] The staging structure is an intermediate phase between $LiFePO_4$ and $FePO_4$ for large crystals or a uniform phase throughout the whole particle for small particles. The distinctive configuration, a thermodynamically metastable but kinetically controlled state, was also explained by density functional theory calculations.[25] The formation of the lithium staging configuration is mainly attributed to the interaction between the effective oxidation state of Fe redox and the arrangement of Li ions.[25] By calculating the magnitude of the overpotential, Ceder *et al.* determined that only minimal overpotential is required to enable the single-phase transformation path of $LiFePO_4$ at room temperature and they explained the difference between larger particles stabilizing intraparticle two-phase coexistence and smaller particles favoring interparticle two-phase coexistence.[26] Kobayashi *et al.* indicated that the particle size determines which primary factor will dominate the electrochemical behavior of $LiFePO_4$.[27] Bulk miscibility dominates the electrochemical behavior of Li_xFePO_4 with particle sizes larger than 40 nm, but the geometric surface portion becomes evident when the particles are smaller than 100 nm.

2.1.2.7 Mechanical strength

Despite the existence of thermodynamic instability, nanometer scale can play yet another favorable role in some aspects of thermodynamic behavior, such as improving the mechanical strength as an excellent strain accommodation during charge/discharge. A plenty of internal cavities or pores can tolerate the volume expansion/contraction associated with lithiation/delithiation. Silicon is an important candidate anode material for the next generation of Li ion batteries because of its extremely high theoretical capacity (4200 mA·h/g), realized by the formation of $Li_{4.4}Si$. However, the reversible capacity of silicon anodes is very poor due to huge volume expansion ($> 300\%$) during the lithiation of silicon, which pulverizes the electrode material, leading to fading capacity. The pulverization of Si resulting from volume changes can be mitigated by integrating particles smaller than 150 nm, as the expansion/contraction of single nanoparticles is much smaller than that of larger particles.[28–31] Li *et al.* reported that a composite of nanoscale silicon power and carbon black exhibits an extremely high reversible capacity of 1700 mA·h/g and excellent cyclic performance.[28] The smaller the particles, the larger the surface-to-volume ratio, accommodating a greater charge and more lithium ions. This fact significantly reduces the lithium ion diffusion distance during charging/discharging, which can greatly reduce the volumetric changes and increase the structural stability, because the structure at the surface is generally more favorable for the diffusion of lithium ions because the diffusion energy of lithium migration is generally higher in the bulk region than near the surface.[32]

The increased reversible capacity of nanomaterials originates both from good structural stability and from new lithium storage mechanisms.

2.1.3. New lithium storage mechanisms

2.1.3.1 Conversion mechanism

One of the new mechanisms is the conversion mechanism, which can be used to explain the excellent lithium storage capacity of nanoscale transition metal oxides, fluorides, sulfides, nitrides, and other polyanion compounds.[33] For amorphous RVO_4 (R = In, Cr, Fe, Al, Y), a model based on the formation of Li–O bonds has been proposed to account for the large Li acceptance that was found in a survey of experimental results.[34] On this basis, Poizot *et al.* reported that the excellent capacity (700 mA·h/g) of nanoscale transition metal oxides MO (M = Co, Ni, Cu, Fe) electrodes stems from the formation/decomposition of Li_2O that occurs with the reduction/oxidation of metal nanoparticles. For transition metals, thermodynamic calculations based on the conversion mechanism for different binary transition metal oxides and fluorides predicted an increase of cell voltage with increasing atomic number.[35]

With the generation of lithiated-state Li_2O or transition metal, the lithium storage capacity is commonly thought to be fully occupied, because it is assumed that the storage material cannot accommodate any more lithium. However, the capacity can be raised further by another lithium storage mechanism (interfacial lithium storage).

2.1.3.2 Interfacial lithium storage mechanism

Interfacial lithium storage mechanism that Li ions and electrons store on the each side of the interface during lithiation process plays a large role in the overall capacity of nanostructural materials due to the comparatively large total interface area of the nanoparticles. *Ab initio* atomic and electronic structure calculations of Ti(0001)/Li_2O(111) indicated that the

interface can store lithium, and a huge transfer of electrons to the Ti adatoms was clearly revealed by 2D difference electron density maps.[36] The interfacial lithium storage mechanism proposed by Jamanik and Maier was confirmed experimentally by the ^{6}Li magic angle spinning nuclear magnetic resonance of the lithiation process of nanocrystalline RuO_2.[37]

2.1.3.3 Lithium storage in nanopores

The third lithium storage mechanism resulting from size reduction is based on the space for lithium ions in the abundant three-dimensional defects such as nanopores or cavities. The size effects might be thought to enhance the properties of electrodes only, yet they also benefit the electrolytes of Li ion batteries.

2.2. Electrolytes

As mentioned above, the practical uses of small materials suffer from intense side reactions and low thermodynamic stability. Solid electrolyte batteries pose a solution, in that the interface between an electrode and a solid electrolyte is more stable. But, solid electrolytes have not been widely used because of their low ionic conductivity and high interfacial resistance. Partial atomic substitution is an effective technique to improve the ionic conductivity, e.g. the substitution of Ge atoms for P atoms in lithium thiophosphate forms $Li_{10}GeP_2S_{12}$, which has unsurpassed ionic conductivity of 1.2×10^{-2} S/cm, however its chemical compatibility with lithium metal is decreased because of the presence of Ge in the structure. Compared with atomic substitution, reduced size is a more feasible strategy for getting high ionic conductivity in solid electrolytes without disrupting chemical stability. For example, Liu *et al.* enhanced room-temperature lithium ion conductivity by three orders of magnitude by creating nanoporous Li_3PS_4, which exists stably in its preferred metastable phase and provides a significant surface conduction mechanism.[38]

Electrolyte composites of liquid non-aqueous salt solutions and solid insulating particles exhibit enhanced conductivity. The phenomenon is attributed to anisotropic forces at the interface between the liquid electrolyte and solid particles, forces which result in space charge areas and dipole effects at high ratio.[39] In the mechanism discussed above, the effect of insulating particles of smaller size is more prominent due to the higher surface-to-volume ratio.

The size effects appearing in Li ion batteries are thought to be caused mainly by the high surface-to-volume ratio, but distortions of atomic or electronic structure at the surface also result in performance changes at a microscopic level. These microscopic changes, difficult to observe in experiment, can be studied by theoretical calculation.

3. The theoretical perspective

Computational methods play a vital role in predicting the structures and properties of materials and suggesting approaches to their modification, all of which are critical for breakthroughs needed for the next generation of Li ion batteries.

3.1. Morphology

It is well known that the morphology of some materials, like the various forms of TiO_2 mentioned above, can have an excellent effect on special properties. To explore the significant enhancement of the surface ratio as the size is reduced, the structural differences between the surface state and bulk state are studied by theoretical calculation.[40–43] The differences are prominent on account of the changes in coordination among the atoms at the surface. The exposed surface orientation and terminations need to be determined at first according to the surface energy difference. Since the difference between the Gibbs energy and the total energy is negligible for solid phases, the surface energy can be calculated by

$$\gamma = (E_{\text{slab}} - E_{\text{bulk}})/2A, \tag{5}$$

where E_{slab} and E_{bulk} are the total energies of the slab and the corresponding bulk, which has the same stoichiometric composition as the slab, and A is the area of the surface.

It is difficult to calculate the surface energy of nonstoichiometric slabs since the chemical potentials need to be considered to determine E_{bulk}. A detailed introduction can be found in Ceder's work.[44]

The equilibrium shape of nanoparticles can be determined according to the surface energies mentioned above by means of Wulff's construction. Seriani *et al.* reported that Li_2O and Li_2O_2 nanoparticles take the forms of octahedra and hexagonal prisms, respectively.[45] Computational techniques can also simulate the process of nucleation, modeling nanoclusters of different sizes, like the reported nanoparticulate oxides and sulfides.[46]

3.2. Electronic structure

The electronic structure of nanoparticles may differ significantly from that of the bulk phase. Changes in the electronic spin state and oxidation state of a cation may appear as the particle size is reduced, due to a decreased ion coordination number at the surface, stemming from surface bonds breaking and reforming. Qian *et al.* reported that electronic spin state transitions occur at the surfaces of stoichiometric $LiCoO_2$, where an intermediate spin state on the square pyramid coordinated site turns into a high spin state on a pseudotetrahedrally coordinated site for trivalent cobalt ions adjacent to the surface.[47] When Co^{3+} near the surface is in either the

intermediate or high spin state explained by the modification of the crystal field splitting of Co(d) orbitals at the surface due to the missed Co–O bonds, the surface energy is decreased and the energy gap between the occupied and unoccupied states of Co ions is also minimized.[47]

The change of electronic state between bulk material and surface structure do not have to be accompanied by the breakage of bonds. Ouyang *et al.* reported that one fourth of Mn ions at the λ-MnO_2 (001) surface undergo a change of oxidation state from +4 to +3 with the surface reconstruction, which does not change the Mn coordination number with oxygen.[48]

3.3. Voltage

Although a voltage change with nanocrystalline can be observed in experiments today, a change in atomic level can be predicted only by theoretical calculations. For nanocrystalline $Li_4Ti_5O_{12}$, Ganapathy *et al.* calculated the Li ion insertion voltage profile of the defective spinel $Li_4Ti_5O_{12}$ and explained the high Li insertion voltage of surface Li storage. Lithium insertion into the subsurface layers of $Li_4Ti_5O_{12}$ (100) (110) and (111) surfaces is allowed at voltages larger than the average insertion voltage. The higher capacities of nanoscale $Li_4Ti_5O_{12}$ can be explained by the fact that (111) surface capacity can exceed bulk capacity. Based on these calculation results, it is predicted that increasing the relative number of (111) facets by reducing the size and tailoring the shape will significantly increase the storage capacity.[49]

3.4. Diffusion coefficient

The improved kinetic performance resulting from nanocrystallization is always explained by shortened diffusion length, but the diffusion coefficient is usually considered to be constant. However, the diffusion coefficient is also affected by a decrease in size in some cases. In one-dimensional diffusion material, diffusion is impeded by the presence of immobile and low-mobility defects in the diffusion path which do not appeared in 2D or 3D diffusion material since the active ion can simply move around the defect. The calculated association between the unblocked capacity fraction and channel length, shown in Fig. 3,[13] suggests that a shorter diffusion channel has more unblocked channels.

Most active ions can diffuse through channels in small particles because most of the channels contain one or zero defects. However, most Li ion sites are not directly accessible from the surface in large materials. If most channels are blocked, the macroscopic diffusion constant is zero according to $D \sim L^2/2\tau$ because τ is a long time. It is suggested that the kinetic benefit of small-particle materials originates from the shortened transport paths and the enhanced diffusion constants of one-dimensional-channel materials whenever point defects are present.[13]

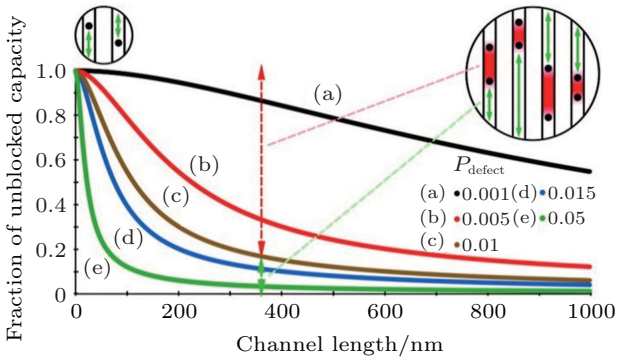


Fig. 3. Predicted association between unblocked capacity and channel length in $LiFePO_4$ for various defect concentrations.[13]

3.5. Mechanisms

The size effects exhibited in battery material can be directly observed in experiment. But the mechanisms behind them are difficult to determine in experiment. So theoretical calculations are used to explain the effects of size on performance, e.g., theoretical calculations about the difference in Li intercalation between bulk β-MnO_2 and nanoscale β-MnO_2. It is difficult to understand why bulk β-MnO_2 can intercalate only a little lithium or none at all, since the migration barrier of Li ions in bulk β-MnO_2 is only 0.17 eV, which one would expect to contribute to good performance as a lithium intercalation cathode. Tompsett *et al.* found that the migration of Li ions in bulk β-MnO_2 is primarily one-dimensional along the *c*-axis tunnels and the route of easy *c*-axis migration is available only at the (101) surface and symmetrical equivalents.[50] The initial barrier to Li ion insertion at the surface is about 0.6 eV, which is the key factor in the intercalation behavior of nanostructured versus bulk β-MnO_2.[50] The superior cyclic stability found in mesoporous or nanoscale β-MnO_2 likely stems from greater exposure of these surfaces.[50]

It is also difficult to understand the varied experimental findings about the phase orientation of $LiFePO_4$ single particles.[51–53] Abdellahi *et al.* pointed out that the varied results originate in that both the chemical interfacial energy and the coherency strain energy scale in different ways with varying particle size (the former being proportional to the interfacial area and the latter to the particle volume), and each may favor different interface orientations.[54] So the phase orientation of $LiFePO_4$ single particles depends upon both particle size and particle morphology.

Although not the focus of this review, it is also worth noting that the size effects described here are exhibited more observably in other energy storage devices[55,56] and other metal ion batteries, such as Na^+ [57–59] and Mg^{2+}.[60,61] It must also be pointed out that some size effects in batteries are not addressed in detail because of the great variation in size effects, such as the degree of difficulty for doping, the special Li insertion sites, and so on.

4. Conclusions and outlook

The differences in materials as size changes have a variety of aspects, such as diffusion length, surface to volume ratio, atomic configuration, and electronic structure. Size effects appear in both the electrodes and electrolytes of Li ion batteries. The performance changes associated with decreasing size may be either advantages (such as enhanced kinetic activity) or disadvantages (such as low thermodynamic stability and intense side reactions). Because of the intense side reactions and low thermodynamic stability, the practical use of small size materials requires both a comprehensive understanding of the size effects and breakthroughs in concepts and technology, such as the realization of all-solid electrolyte batteries with their more stable electrode–electrolyte interface. For contemporary studies of the mechanism behind the size effects, the combination of experimental means and computational techniques has become vital, as the microscopic distinctions are difficult to observe through conventional experimental measurements. Understanding various size effects and mechanisms requires more research from a range of disciplines, and it would lead to genuine development of nanoscale or other size materials and then promote progress toward a new generation of Li ion batteries with a leap in either energy density or power density.

References

[1] Maier J 2005 *Nat. Mater.* **4** 805
[2] Wu X L, Jiang L Y, Cao F F, Guo Y G and Wan L J 2009 *Adv. Mater.* **21** 2710
[3] Wu X L, Guo Y G, Su J, Xiong J W, Zhang Y L and Wan L J 2013 *Advanced Energy Materials* **3** 1155
[4] Yang J, Han X, Zhang X, Cheng F and Chen J 2013 *Nano Research* **6** 679
[5] Hu Y S, Kienle L, Guo Y G and Maier J 2006 *Adv. Mater.* **18** 1421
[6] Feng G X, Li L F, Liu J Y, Liu N, Li H, Yang X Q, Huang X J, Chen L Q, Nam K W and Yoon W S 2009 *Journal of Materials Chemistry* **19** 2993
[7] Yu X Y, Bin Wu H, Yu L, Ma F X and Lou X W 2015 *Angewandte Chemie-International Edition* **54** 4001
[8] Pfanzelt M, Kubiak P, Fleischhammer M and Wohlfahrt-Mehrens M 2011 *Journal of Power Sources* **196** 6815
[9] Ouyang C Y, Zhong Z Y and Lei M S 2007 *Electrochemistry Communications* **9** 1107
[10] Prakash A S, Manikandan P, Ramesha K, Sathiya M, Tarascon J M and Shukla A K 2010 *Chemistry of Materials* **22** 2857
[11] Zhang B, Liu Y, Huang Z, Oh S, Yu Y, Mai Y W and Kim J K 2012 *Journal of Materials Chemistry* **22** 12133
[12] Zhao Y, Peng L, Liu B and Yu G 2014 *Nano. Lett.* **14** 2849
[13] Malik R, Burch D, Bazant M and Ceder G 2010 *Nano. Lett.* **10** 4123
[14] Liu N, Li H, Wang Z X, Huang X J and Chen L Q 2006 *Electrochemical and Solid State Letters* **9** A328
[15] Okubo M, Hosono E, Kim J, Enomoto M, Kojima N, Kudo T, Zhou H and Honma I 2007 *J. Am. Chem. Soc.* **129** 7444
[16] Zhang W M, Wu X L, Hu J S, Guo Y G and Wan L J 2008 *Advanced Functional Materials* **18** 3941
[17] Guo Y G, Hu Y S, Sigle W and Maier J 2007 *Adv. Mater.* **19** 2087
[18] Wu L J, Wiesmann H J, Moodenbaugh A R, Klie R F, Zhu Y M, Welch D O and Suenaga M 2004 *Phys. Rev. B* **69** 125415
[19] Tsunekawa S, Ito S, Mori T, Ishikawa K, Li Z Q and Kawazoe Y 2000 *Phys. Rev. B* **62** 3065
[20] Balaya P and Maier J 2010 *Physical Chemistry Chemical Physics* **12** 215
[21] Gibot P, Casas-Cabanas M, Laffont L, Levasseur S, Carlach P, Hamelet S, Tarascon J M and Masquelier C 2008 *Nat. Mater.* **7** 741
[22] Zhu C, Mu X, Popovic J, Weichert K, van Aken P A, Yu Y and Maier J 2014 *Nano. Lett.* **14** 5342
[23] Schimanke G and Martin M 2000 *Solid State Ionics* **136** 1235
[24] Zhu C, Gu L, Suo L, Popovic J, Li H, Ikuhara Y and Maier J 2014 *Advanced Functional Materials* **24** 312
[25] Sun Y, Lu X, Xiao R, Li H and Huang X 2012 *Chemistry of Materials* **24** 4693
[26] Malik R, Zhou F and Ceder G 2011 *Nat. Mater.* **10** 587
[27] Kobayashi G, Nishimura S i, Park M S, Kanno R, Yashima M, Ida T and Yamada A 2009 *Advanced Functional Materials* **19** 395
[28] Li H, Huang X J, Chen L Q, Wu Z G and Liang Y 1999 *Electrochemical and Solid State Letters* **2** 547
[29] Liu B, Soares P, Checkles C, Zhao Y and Yu G 2013 *Nano. Lett.* **13** 3414
[30] Piper D M, Travis J J, Young M, Son S B, Kim S C, Oh K H, George S M, Ban C and Lee S H 2014 *Adv. Mater.* **26** 1596
[31] Ko M, Chae S, Jeong S, Oh P and Cho J 2014 *Acs Nano* **8** 8591
[32] Ma H, Ji W Q, Yang X J, Tao Z L and Chen J 2009 *Science in China. Series B, Chemistry* **39** 918
[33] Chen J, Xu L N, Li W Y and Gou X L 2005 *Adv. Mater.* **17** 582
[34] Denis S, Baudrin E, Touboul M and Tarascon J M 1997 *Journal of the Electrochemical Society* **144** 4099
[35] Li H, Balaya P and Maier J 2004 *Journal of the Electrochemical Society* **151** A1878
[36] Zhukovskii Y F, Balaya P, Kotomin E A and Maier J 2006 *Phys. Rev. Lett.* 96
[37] Bekaert E, Balaya P, Murugavel S, Maier J and Menetrier M 2009 *Chemistry of Materials* **21** 856
[38] Liu Z, Fu W, Payzant E A, Yu X, Wu Z, Dudney N J, Kiggans J, Hong K, Rondinone A J and Liang C 2013 *J. Am. Chem. Soc.* **135** 975
[39] Bhattacharyya A J and Maier J 2004 *Adv. Mater.* **16** 811
[40] Whiteside A, Fisher C A J, Parker S C and Islam M S 2014 *Physical Chemistry Chemical Physics* **16** 21788
[41] Andreev Y G, Panchmatia P M, Liu Z, Parker S C, Islam M S and Bruce P G 2014 *J. Am. Chem. Soc.* **136** 6306
[42] Barnard A S and Zapol P 2004 *Journal of Physical Chemistry B* **108** 18435
[43] Moriguchi K, Munetoh S, Abe M, Yonemura M, Kamei K, Shintani A, Maehara Y, Omaru A and Nagamine M 2000 *J. Appl. Phys.* **88** 6369
[44] Kramer D and Ceder G 2009 *Chemistry of Materials* **21** 3799
[45] Seriani N 2009 *Nanotechnology* 20
[46] Catlow C R A, Bromley S T, Hamad S, Mora-Fonz M, Sokol A A and Woodley S M 2010 *Physical Chemistry Chemical Physics* **12** 786
[47] Qian D, Hinuma Y, Chen H, Du L S, Carroll K J, Ceder G, Grey C P and Meng Y S 2012 *J. Am. Chem. Soc.* **134** 6096
[48] Ouyang C Y, Sljivancanin Z and Baldereschi A 2010 *Journal of Chemical Physics* 133
[49] Ganapathy S and Wagemaker M 2012 *Acs Nano* **6** 8702
[50] Tompsett D A, Parker S C, Bruce P G and Islam M S 2013 *Chemistry of Materials* **25** 536
[51] Park S B, Park C K, Hwang J T, Cho W I and Jang H 2011 *Metals and Materials International* **17** 1017
[52] Suo L, Han W, Lu X, Gu L, Hu Y S, Li H, Chen D, Chen L, Tsukimoto S and Ikuhara Y 2012 *Physical Chemistry Chemical Physics* **14** 5363
[53] Zhu Y, Wang J W, Liu Y, Liu X, Kushima A, Liu Y, Xu Y, Mao S X, Li J, Wang C and Huang J Y 2013 *Adv. Mater.* **25** 5461
[54] Abdellahi A, Akyildiz O, Malik R, Thornton K and Ceder G 2014 *Journal of Materials Chemistry A* **2** 15437
[55] Naoi K, Naoi W, Aoyagi S, Miyamoto J I and Kamino T 2013 *Accounts of Chemical Research* **46** 1075
[56] Zhang W D, Xu B and Jiang L C 2010 *Journal of Materials Chemistry* **20** 6383
[57] Cao Y, Xiao L, Wang W, Choi D, Nie Z, Yu J, Saraf L V, Yang Z and Liu J 2011 *Adv. Mater.* **23** 3155
[58] Pan H, Lu X, Yu X, Hu Y S, Li H, Yang X Q and Chen L 2013 *Advanced Energy Materials* **3** 1186
[59] Kim J, Seo D H, Kim H, Park I, Yoo J K, Jung S K, Park Y U, Goddard W A III and Kang K 2015 *Energy & Environmental Science* **8** 540
[60] Wu N, Lyu Y C, Xiao R J, Yu X, Yin Y X, Yang X Q, Li H, Gu L and Guo Y G 2014 *Npg Asia Materials* **6** e120
[61] Wu N, Yang Z Z, Yao H R, Yin Y X, Gu L and Guo Y G 2015 *Angewandte Chemie-International Edition* **54** 5757